

## Effect of CuCr<sub>1</sub>Zr Cross-Contamination Level on Work Hardening Characteristics of AlSi<sub>10</sub>Mg Additive Manufactured Material

Ioanna Giavrouta<sup>1,a\*</sup>, Max Horn<sup>2,b</sup>, Leonard Alberty<sup>2,c</sup>, Ismail Ünsal<sup>2,d</sup>, Georg Schlick<sup>2,e</sup> and Nikolaos D. Alexopoulos<sup>1,f</sup>

<sup>1</sup>University of the Aegean, School of Engineering, Department of Financial and Management Engineering, Research Unit of Advanced Materials, 41 Kountouriotou str, 82132, Chios, Greece

<sup>2</sup>Fraunhofer-Institut für Gießerei-, Composite- und Verarbeitungstechnik IGCV, Am Technologiezentrum 10 | 86159 Augsburg

\*fme21021@fme.aegean.gr, <sup>b</sup>max.horn@igcv.fraunhofer.de, <sup>c</sup>leonard.alberty@igcv.fraunhofer.de, <sup>d</sup>ismail.uensal@igcv.fraunhofer.de, <sup>e</sup>georg.schlick@igcv.fraunhofer.de, <sup>f</sup>nalexop@aegean.gr

**Keywords:** additive manufacturing, metallic multi-material 3D printing, work-hardening.

**Abstract.** Cross-contamination occurring after the blending of metal powders in multi-material laser powder bed fusion (PBF-LB/M) is a frequent manufacturing issue and poses a major obstacle to the further development of this emerging additive manufacturing process. To evaluate the influence of such contamination on a technologically important material system for multi-material PBF-LB/M, this study investigates the impact of CuCr<sub>1</sub>Zr foreign particle contamination within AlSi<sub>10</sub>Mg powder on the resulting metallurgical characteristics and mechanical performance of the fabricated parts. Several contamination levels of CuCr<sub>1</sub>Zr were considered, namely 0.5 wt.%, 3.0 wt.% and 5.0 wt.%, with the results benchmarked against samples produced from uncontaminated powder. Tensile testing demonstrated that the cross-contamination contribute to material embrittlement. This investigation focuses on the tensile work-hardening behaviour of the investigated materials showcasing that the specimens exhibit only the first two work-hardening stages, while for the higher contamination level studied, the material becomes brittle and fractures even in the first work hardening stage.

### Introduction

Multi-material laser powder bed fusion (PBF-LB/M) is gaining recognition as a promising additive manufacturing method that addresses the rising need for high-precision metallic components, while minimizing production times and enhancing sustainability. This technique proves particularly valuable for aerospace and automotive sectors, where material diversity and the fabrication of intricate geometries are critical requirements. However, powder cross-contamination continues to pose a primary obstacle to its widespread industrial implementation.

Even minimal contamination levels, especially involving dissimilar metals, can cause significant deterioration in mechanical properties, structural integrity, and functional performance of the produced components. In automotive applications, bi-metallic additive manufacturing presents unique challenges, commonly requiring the integration of aluminium alloys with chromium-zirconium-copper alloys.

This present investigation focuses on the impact of CuCr<sub>1</sub>Zr particle contamination on AlSi<sub>10</sub>Mg powder feedstock. Previous studies on additively manufactured AlSi<sub>10</sub>Mg have highlighted the critical role of the cellular microstructure and melt pool boundaries in governing strain hardening and mechanical performance [1]. Approaches based on retaining the AlSi<sub>10</sub>Mg cell network through direct aging have been shown to offer advantages compared to conventional T6 heat treatment, which relies primarily on precipitation strengthening [2]. Prior research has established that powder contamination modifies the microstructure of additively manufactured components and adversely affects critical mechanical properties, including tensile strength, ductility, and fatigue resistance [3]. The presence of copper-based contaminant particles is expected to alter strain hardening characteristics through local heterogeneities, modified load transfer mechanisms and potential stress

concentration sites. Work hardening constitutes a critical mechanical response, as it governs the material's ability to accommodate plastic deformation and directly affects strength, ductility and damage tolerance [4]. Variations in work hardening behaviour are often indicative of underlying changes in microstructural mechanisms such as dislocation density, phase distribution and interfacial interactions induced by foreign particle incorporation.

Building upon the considerations, the present study specifically focuses on the work hardening behaviour of AlSi10Mg components fabricated via PBF-LB/M and the influence of CuCr1Zr powder cross-contamination on this phenomenon. By analysing the evolution of work hardening parameters derived from tensile testing, this study aims to elucidate the role of powder cross-contamination in governing plastic deformation mechanisms and overall mechanical performance of PBF-LB/M fabricated components.

## Experimental Procedure

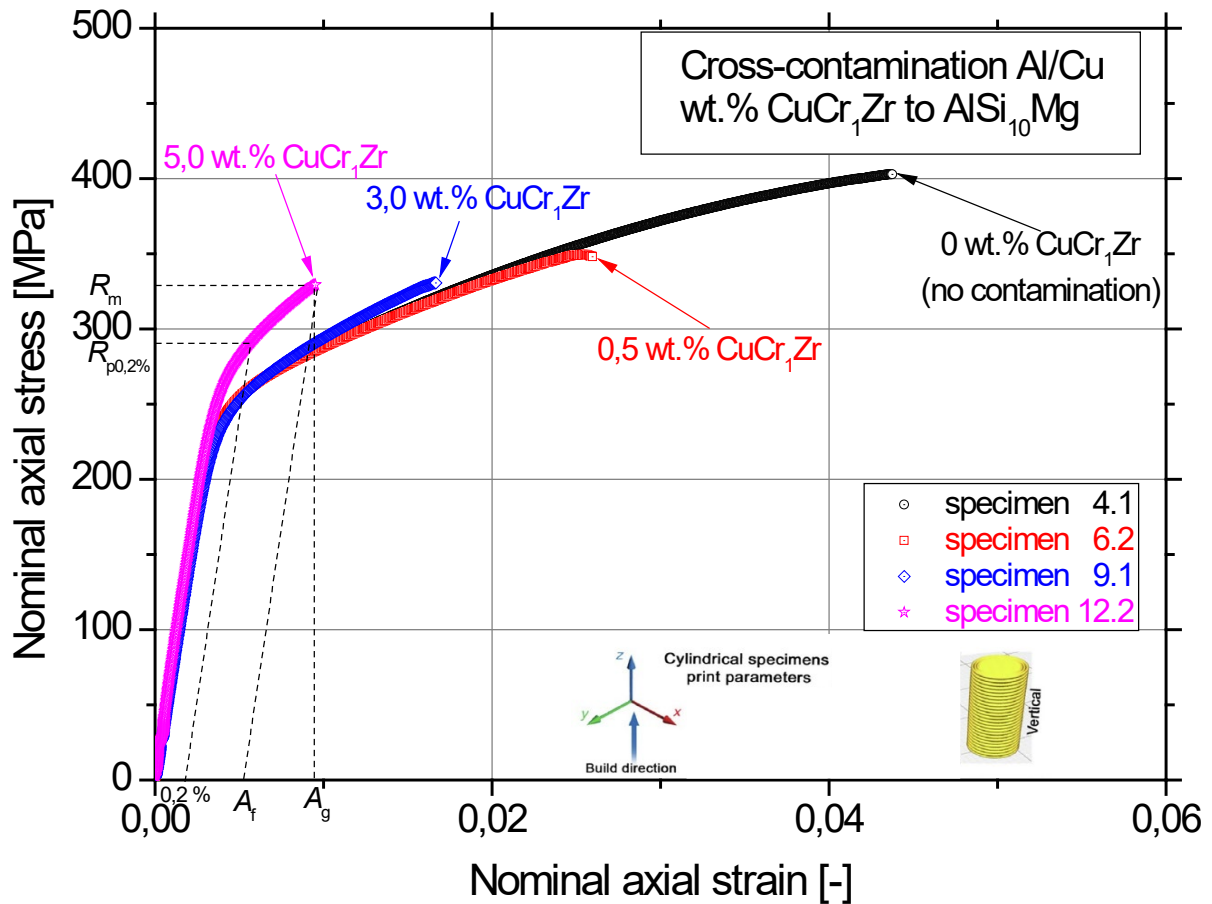
The aluminium alloy EN AC-43000 (AlSi10Mg) served as the matrix material. This precipitation-hardenable cast alloy exhibits good electrical conductivity and high chemical resistance in corrosive environments (DIN EN 1706:2013). Owing to its excellent compatibility with laser powder bed fusion (PBF-LB/M) and its high specific strength, AlSi10Mg represents the most utilized aluminium alloy in this additive manufacturing process (SLM Solutions, 2019). Powder supplied by SLM Solutions Group AG, featuring a particle size distribution of +20/−63  $\mu\text{m}$ , was employed in this study.

The copper alloy CW106C (CuCr1Zr) was chosen as the contaminant material. Alloying copper with chromium (Cr) and zirconium (Zr) enhances mechanical strength, thermal stability, and wear resistance while substantially maintaining high electrical and thermal conductivity (German Copper Alliance, 2005). The CuCr1Zr powder, with a particle size range of +20/−45  $\mu\text{m}$ , was provided by Schmelzmetall GmbH. Particle size distributions for both powders were characterized using a Mastersizer 3000 (Malvern Panalytical Ltd.).

Tensile tests were conducted to evaluate the mechanical behaviour of AlSi10Mg specimens fabricated by multi-material PBF-LB/M with different degrees of CuCr1Zr powder cross-contamination. Cylindrical specimens were manufactured according to DIN 50125 – B4 x 20 standard with 4 mm diameter at the reduced cross-section. During mechanical testing, axial load and axial deformation were continuously recorded, allowing the calculation of engineering stress–strain curves for each specimen. The recorded engineering stress–strain data were subsequently converted into true (nominal axial) stress–strain curves to account for the continuous reduction of the cross-sectional area during plastic deformation. This conversion enabled a more accurate determination of the conventional yield stress and ultimate tensile strength, as well as a more representative description of the material response under tensile loading. Conventional yield stress was determined using the 0.2% offset method, while the ultimate tensile strength was defined as the maximum stress reached prior to fracture. The stress–strain data obtained up to uniform elongation were further used for the evaluation of work hardening behaviour.

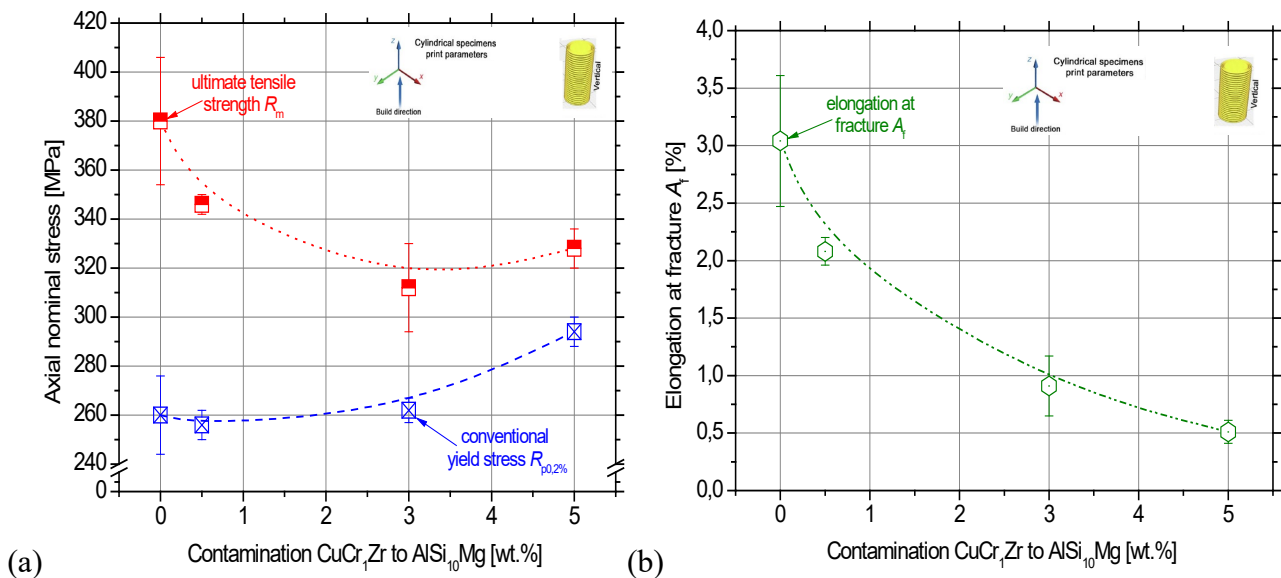
## Results and Discussion

Fig. 1 presents typical nominal axial tensile stress–strain curves of additively manufactured AlSi10Mg specimens fabricated in the upright ( $0^\circ$ ) build direction for different levels of CuCr1Zr powder cross-contamination. Specimens containing 3 wt.% and 5 wt.% CuCr1Zr display a noticeably steeper stress–strain response and premature fracture, indicating increasing material embrittlement induced by powder cross-contamination.



**Fig. 1.** Nominal axial tensile stress-strain curves of additively manufactured AlSi10Mg specimens printed at upright ( $0^\circ$ ) building direction for different levels of CuCr<sub>1</sub>Zr cross-contamination.

The influence of contamination level on the conventional yield stress ( $R_{p0.2\%}$ ) and ultimate tensile strength ( $R_m$ ) is summarized in Fig. 2a and 2b, respectively. A moderate increase in conventional yield stress is observed with increasing CuCr<sub>1</sub>Zr contamination. In contrast, the ultimate tensile strength shows a decreasing trend (15 % maximum decrease) for the higher investigated contamination levels.



**Fig. 2.** (a) Effect of different wt.% CuCr<sub>1</sub>Zr cross-contamination on the conventional yield stress  $R_{p0.2\%}$  and (b) ultimate tensile strength  $R_m$  of additively manufactured AlSi<sub>10</sub>Mg specimens printed at upright ( $0^\circ$ ) building direction.

The work hardening behaviour of uncontaminated additively manufactured AlSi10Mg specimens is illustrated in Fig. 3. It is characterized by the presence of two distinct work hardening stages and the slopes gives the respective strain hardening exponents  $n_I$  and  $n_{II}$ . For low and moderate levels of CuCr1Zr powder cross-contamination, both stages are clearly identifiable between the conventional yield point and the onset of necking. However, at high contamination levels, the material exhibits pronounced brittle behaviour, and fracture occurs prematurely during the first work hardening stage, preventing the development of the second stage.

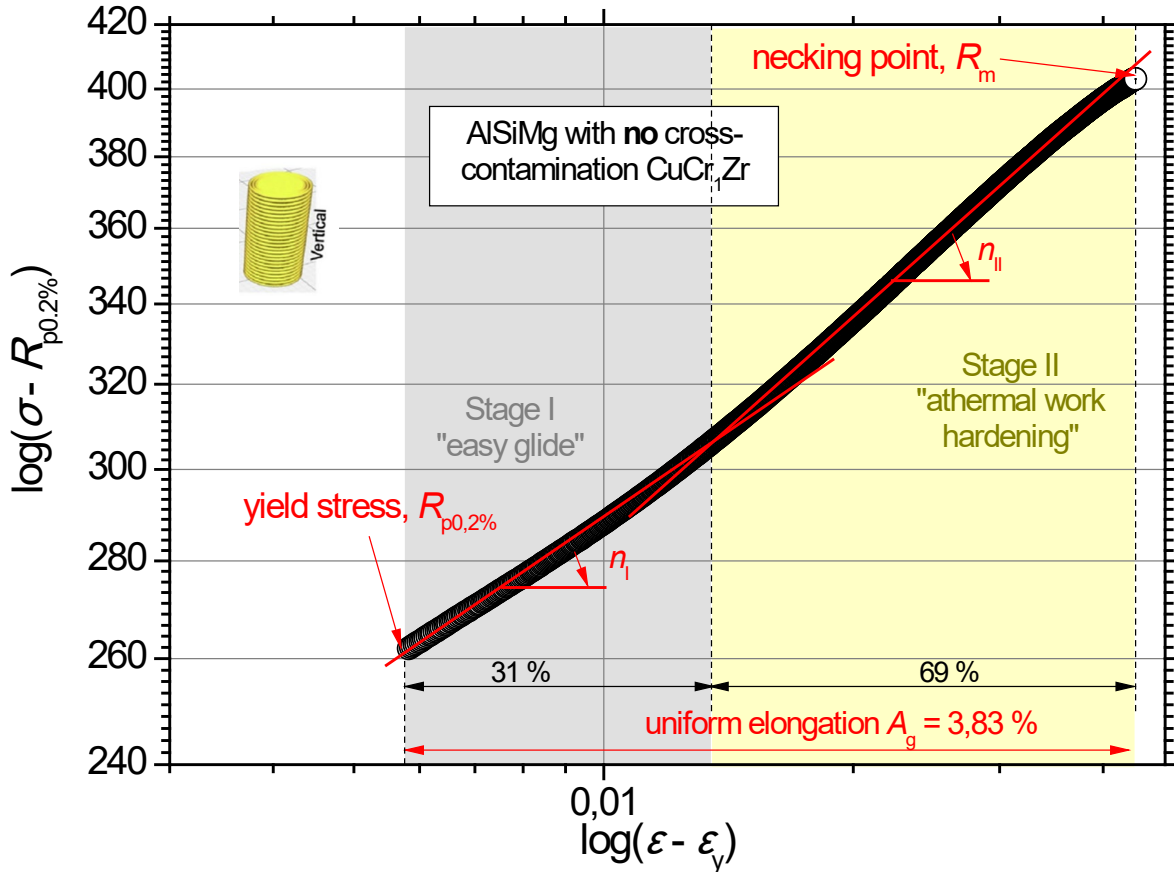


**Fig. 3.** Image showing the evaluation of the work hardening behaviour, showcasing the work hardening stages and strain hardening exponents ( $n_I$  and  $n_{II}$ ) from conventional yield stress point ( $R_{p0.2\%}$ ) till necking point ( $R_m$ ) for additively manufactured AlSi10Mg specimen printed at upright ( $0^\circ$ ) building direction without CuCr1Zr cross-contamination.

Fig. 4a summarizes the dependence of the strain hardening exponents  $n_I$  and  $n_{II}$  on CuCr1Zr contamination level. The strain hardening exponent  $n_I$ , associated with stage I, increases systematically from approximately 0.18 for uncontaminated material and rises in an almost linear manner up to about 0.22 for the highest CuCr1Zr cross-contamination level. In contrast,  $n_{II}$  exhibits a decreasing tendency with increasing contamination, indicating a reduced capacity for sustained plastic deformation at higher strain levels. Similar results were noticed [5-7] for contaminated and non-contaminated PBF-LB/M -fabricated AlSi10Mg material.

The relative contribution of each work hardening stage to the total uniform elongation is shown in Fig. 4b. For low contamination levels, both work hardening stages contribute significantly to the overall plastic deformation. However, as the CuCr1Zr contamination increases, the contribution of stage II diminishes markedly, and for the highest contamination level, fracture occurs predominantly during stage I. This behaviour confirms that high levels of powder cross-contamination promote premature failure.

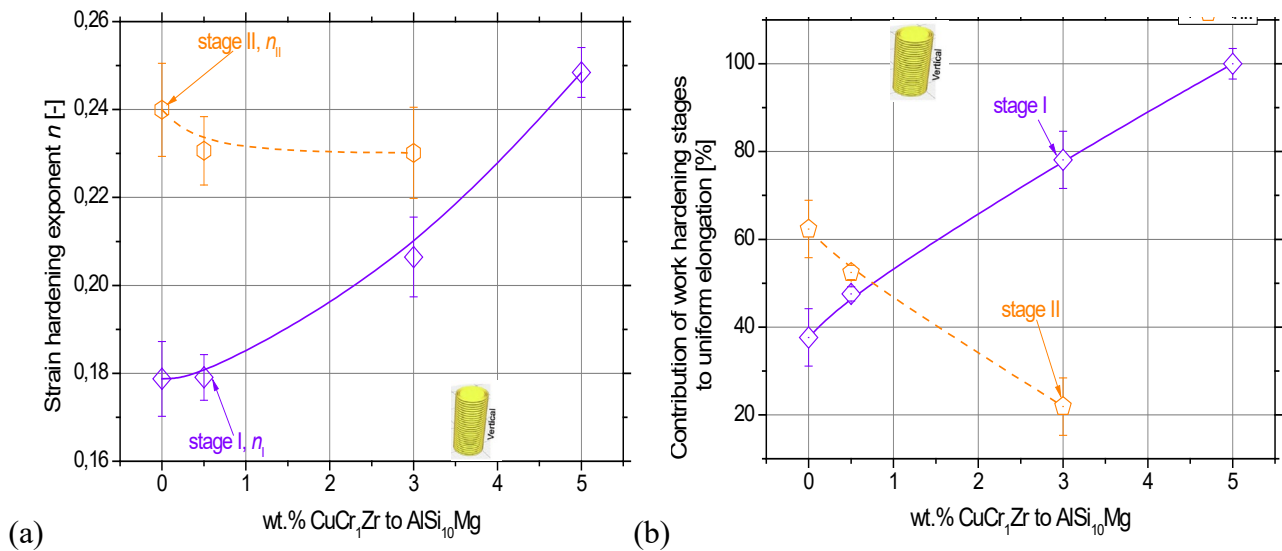


**Fig. 4.** (a) Dependence of strain hardening exponents  $n_I$  and  $n_{II}$  from stage I and stage II, respectively as well as (b) relative contribution of the work hardening stages to uniform elongation for different CuCr<sub>1</sub>Zr cross-contamination in AlSi<sub>10</sub>Mg tensile specimens at 0° building direction.

Overall, the results demonstrate that CuCr<sub>1</sub>Zr powder cross-contamination has a pronounced effect on the tensile and work hardening behaviour of PBF-LB/M -fabricated AlSi<sub>10</sub>Mg. While higher contamination levels severely compromise tensile ductility and strain hardening capacity, ultimately resulting in brittle fracture.

## Summary

The currently available results identify that the cross-contamination plays a significant role in the tensile mechanical behaviour as well as to the respective tensile work hardening behaviour. The results showed that a maximum decrease of 15 % in ultimate tensile strength is shown, while more than 80 % decrease in tensile elongation at fracture was noticed for the higher cross-contamination level investigated. As far as the work hardening behaviour is concerned, the work hardening stages are reduced from four to only two, due to the observed pre-mature fracture of the specimens. The work-hardening exponent ranges from 0.18 for non-contaminated material to almost 0.25 for the highly contaminated material, showcasing that work-hardening is strongly affected by the cross-contamination level.

## Acknowledgement

The authors gratefully acknowledge the financial support of the HORIZON Research and Innovation Actions, European Health and Digital Executive Agency for the implementation of the project «MULTI-MATERIAL DESIGN USING 3D PRINTING» having an acronym “MADE-3D” of the act HORIZON-CL4-2022-RESILIENCE-01 with Grant Agreement code 101091911.

## References

- [1] E. Cerri, E. Ghio, On the work-hardening behaviour of the additively manufactured Al-Si-Mg alloys: Composite-like versus networked microstructure, *Materialia* 38 (2024) 102282.
- [2] J. Fite, S. E. Prameela, J. Slotwinski, T. P. Weihs, Enhanced mechanical properties by eutectic cells in AlSi<sub>10</sub>Mg – A promising paradigm for strengthening aluminum in additive manufacturing, *Mater. Charact.*, 204, (2023).
- [3] M. Horn, G. Schlick, M. Lutter-Guenther, C. Anstaett, C. Seidel, G. Reinhart, Metal powder cross-contaminations in multi-material laser powder bed fusion: Influence of CuCr<sub>1</sub>Zr particles in AlSi<sub>10</sub>Mg feedstock on part properties, (LiM 2019), (2019).

- [4] N. D. Alexopoulos & M. Tiryakioğlu, Relationship between fracture toughness and tensile properties of A357 cast aluminum alloy, *MMTA*, 40, (2009), 702–716.
- [5] C. Li, W.X. Zhang, H.O. Yang, J. Wan, X.X. Huang, Y.Z. Chen, Microstructural origin of high strength and high strain hardening capability of a laser powder bed fused AlSi10Mg alloy, *J. Mat. Sci. Technol.* 197 (2024), 194–206.
- [6] M. Avateffazeli, S. I. Shakil, A. Hadadzadeh, B. Shalchi-Amirkhiz, H. Pirgazi, M. Mohammadi, M. Haghshenas, On microstructure and work hardening behavior of laser powder bed fused Al-Cu-Mg-Ag-TiB<sub>2</sub> and AlSi10Mg alloys, *Mater. Today Commun.*, 35 (2023) 105804.
- [7] R. Ramesh, S. Gairola, R. Jayaganthan, M. Kamaraj, Effects of post-processing on the microstructural evolution and mechanical behaviour of an additively manufactured AlSi10Mg alloy, *J. Mat. Res. Technol.* 34, (2025), 2802–2813.